Electric Sail Elliptic Displaced Orbits with Advanced Thrust Model

Lorenzo Niccolai, Alessandro A. Quarta*, Giovanni Mengali

Department of Civil and Industrial Engineering, University of Pisa, I-56122 Pisa, Italy

Abstract

This paper analyzes the performance of an Electric Solar Wind Sail for generating and maintaining an elliptic, heliocentric, displaced non-Keplerian orbit. In this sense, this paper extends and completes recent studies regarding the performances of an Electric Solar Wind Sail that covers a circular, heliocentric, displaced orbit of given characteristics. The paper presents the general equations that describe the elliptic orbit maintenance in terms of both spacecraft attitude and performance requirements, when a refined thrust model (recently proposed for the preliminary mission design) is taken into account. In particular, the paper also discusses some practical applications on particular mission scenarios in which an analytic solution of the governing equations has been found.

Keywords: Electric solar wind sail, elliptic displaced orbits, mission analysis

Nomenclature

$\boldsymbol{a}$	=	propulsive acceleration, [mm/s^2]
a_c	=	spacecraft characteristic acceleration, [mm/s^2]
a	=	planet's orbit semimajor axis, [au]
a_ρ, a_z	=	components of the propulsive acceleration, [mm/s^2]
d	=	planet-spacecraft distance, [au]
e	=	planet's orbit eccentricity
H	=	vertical displacement of non-Keplerian orbit, [au]
h_z	=	vertical component of the spacecraft specific angular momentum, [au^2/TU]
$\hat{\boldsymbol{n}}$	=	unit vector normal to the E-sail mean plane
O	=	Sun's center-of-mass
O'	=	projection of Sun's center-of-mass on the DNKO plane
P	=	perihelion of the planet's orbit
P'	=	pericenter of the displaced orbit
q	=	ratio of spacecraft radial coordinate to planet's heliocentric distance
$\boldsymbol{r}$	=	spacecraft position vector (with $r \triangleq \|\boldsymbol{r}\|$), [au]
r_p	=	planet's heliocentric distance, [au]
$r_\oplus$	=	reference distance (1 au)
S	=	spacecraft center-of-mass
z	=	spacecraft vertical coordinate, [au]
α	=	cone angle, [deg]
α_n	=	pitch angle, [deg]
γ	=	dimensionless propulsive acceleration

*Corresponding author

Email addresses: lorenzoniccolai88@gmail.com (Lorenzo Niccolai), a.quarta@ing.unipi.it (Alessandro A. Quarta), g.mengali@ing.unipi.it (Giovanni Mengali)

Published in Acta Astronautica, online before print, November 2016. doi: http://dx.doi.org/10.1016/j.actaastro.2016.10.036

$\mu_\odot$ = Sun's gravitational parameter, [km^3/s^2]
ν = planet's true anomaly, [deg]
ω = angle between spacecraft and planet apse line, [deg]
ψ = elevation angle, [deg]
ρ = spacecraft radial coordinate, [au]
τ = voltage parameter
θ = spacecraft angular coordinate, [deg]

Subscripts

max = maximum
min = minimum

Superscripts

$\cdot$ = time derivative
$\wedge$ = unit vector

1. Introduction

The Electric Solar Wind Sail (E-sail) is a recent, propellantless, propulsion system concept [1, 2, 3] that consists of a number of thin, long, and conducting tethers, which are deployed and stretched out using the centrifugal force obtained by spinning the spacecraft around its symmetry axis [4]. The tethers, which are kept at a high positive potential by an onboard electron gun, experience Coulomb drag [5] by interacting with the solar wind plasma stream and generate a propulsive thrust [6, 7]. The E-sail is theoretically able to allow a spacecraft to reach and maintain highly non-Keplerian orbits, which are difficult, or even impossible, to be generated with more conventional propulsion systems such as chemical or electrical thrusters [8]. Within this set of highly non-Keplerian closed trajectories, a class of great practical importance is that of displaced orbit, whose orbital plane does not contain the primary body.

The concept of displaced non-Keplerian orbit (DNKO) has received a great interest in the recent scientific literature [9, 10]. Most of the available studies involve the use of a photonic solar sail as the propulsion system for orbital maintenance. An excellent survey of the potential applications for DNKOs can be found in the comprehensive survey by McKay et al. [11].

This paper, instead, focuses on DNKOs maintained by an E-sail. A preliminary analysis of such a subject has been given in Ref. [12]. However, that study [12] was based on a simplified mathematical model of the E-sail performance, characterized by two main assumptions. On one side the thrust modulus variation with the Sun-spacecraft distance r was chosen proportional to $1/r^{7/6}$, whereas more recent plasmadynamic simulations [13] have shown that the thrust modulus scales as the inverse of the Sun-spacecraft distance, i.e. as $1/r$. The second simplified assumption used in Ref. [12] was that the propulsive acceleration was assumed to be independent of the spacecraft attitude and the thrust direction formed an angle (the cone angle) approximatively equal to one half of the angle between the Sun-spacecraft line and the normal to the sail plane (the pitch angle). In a recent paper Yamaguchi and Yamakawa [14] have proposed a more accurate mathematical model in which the thrust modulus and direction are both parameterized as functions of the E-sail attitude. The refined thrust model has been used in Ref. [15] to analyze the E-sail performances in an asteroid deflection mission, and in Ref. [16] for studying circular DNKOs in an E-sail-based interplanetary scenario.

The aim of this paper is to extend the results of Ref. [16] to the more general (and complex) case of elliptic heliocentric DNKOs using, again, the refined thrust model by Yamaguchi and Yamakawa [14]. In fact, an interesting potential application of an elliptic DNKO is the observation of the polar regions of a planet or, in general, of a celestial body. The paper starts by looking for the values of thrust modulus and direction necessary to maintain a generic, elliptic, DNKO. In this context, the thrust modulus variation along the orbit, due to the time variation of the spacecraft-focus distance, can be obtained by suitably adjusting the E-sail tether voltage [4, 17].

Some special mission scenarios are discussed, in particular the case of a planet following displaced orbit in which the E-sail-based spacecraft moves along the displaced orbit with the same angular velocity of a reference planet. In this case, the DNKO eccentricity is assumed to be equal to that of the planetary orbit, but the semimajor axes of the two orbits can be different in order to obtain a parametric study of this scenario. Indeed, the ratio of the two semimajor axes and the amount of displacement (with respect to the planet's orbital plane) are two fundamental parameters that must be carefully chosen in order to obtain a feasible DNKO.

The paper is organized as follows. The next section presents the mathematical model that has been used for the analysis of the spacecraft performances in a (general) heliocentric, elliptic, displaced orbit. Section III introduces the concept of a particular displaced heliocentric orbit and illustrates, through numerical simulations, the E-sail capabilities in some interesting mission scenario. Finally, the Conclusion section presents the outcome of this work.

2. Mathematical model

Consider a planet's heliocentric orbit as a reference (Keplerian) orbit and introduce a classical, perifocal, reference frame $\mathcal{T}(O; x, y, z)$, see Fig. 1.

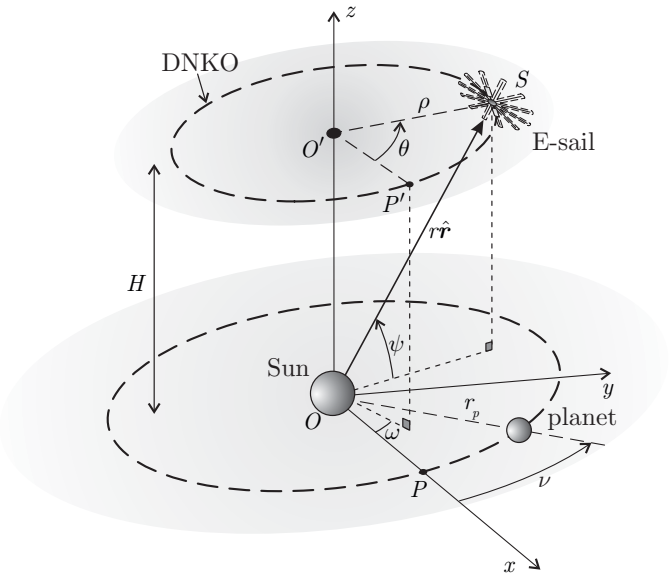

Figure 1: Reference frame and DNKO schematic view.

The origin of $\mathcal{T}$ is at the Sun's center-of-mass O, the plane (x, y) coincides with the orbital plane (the x-axis points towards the celestial body's perihelion P), and the z-axis is orthogonal to the orbital plane in the direction of the planet's angular momentum vector. The planet's position along the orbit is given by its true anomaly ν, measured counterclockwise from the x-axis. Assume that the DNKO orbital plane is parallel to the (x, y) plane, and is placed at a (given) distance H with respect to the Sun's center of mass O. Moreover, the DNKO primary focus O' is assumed to coincide with the orthogonal projection of O onto the DNKO plane, whereas P' is the DNKO perihelion where the O'-spacecraft distance is minimum, see Fig. 1.

The spacecraft position S along the DNKO orbit is conveniently described by a cylindrical coordinate system $\mathcal{T}_c\,(O'; \rho, \theta, z)$, where ρ coincides with the O'-S distance, and θ is the spacecraft angular coordinate measured counterclockwise starting from the O'-P' direction. Note that, by definition, ν and θ differ for a constant angle ω that coincides with the angle between the x-axis and the O'-P' direction, see Fig. 1.

To maintain an elliptic DNKO, the spacecraft needs to be equipped with a propulsion system capable of providing a continuous and, within some limits, adjustable thrust. To that aim, in principle the spacecraft could use a propulsion system that exploits some kind of propellant to generate the required continuous

thrust, such as a classical electric thruster. However, if the spacecraft is planned to track a DNKO for a long time interval, on the order of several months or years, the only feasible option is to resort to a propellantless propulsion system, which removes the constraint involving the finite amount of available propellant. Taking into account the current technology level, the natural choice is confined to either a photonic solar sail, or to the more recent E-sail. Unlike the former, the latter enables a simpler thrust modulation to be obtained by adjusting the tether voltage.

Accordingly, this paper assumes that the spacecraft is equipped with an E-sail whose more recent thrust model has been introduced by Yamaguchi and Yamakawa [14] and thoroughly analyzed, for a minimum-time heliocentric-transfer mission scenario, in a recent paper by Quarta and Mengali [18]. To summarize the advanced thrust model [14] conveniently, let $\hat{\boldsymbol{n}}$ be the unit vector normal to the nominal plane containing the E-sail tethers, in the direction opposite to the Sun. According to Refs. [14, 18], the E-sail propulsive acceleration vector $\boldsymbol{a}$ is a suitable function of both the Sun-spacecraft distance r, and the sail pitch angle $\alpha_n \in [0,\, 90]\,\mathrm{deg}$, defined as the angle between the direction of $\hat{\boldsymbol{n}}$ and the direction of the spacecraft position unit vector $\hat{\boldsymbol{r}}$ (i.e. the direction of the spacecraft position vector measured from O), viz.

$$\boldsymbol{a} = \tau\, a_c \left(\frac{r_\oplus}{r}\right) \gamma\, \hat{\boldsymbol{a}} \tag{1}$$

where a_c is the spacecraft characteristic acceleration, defined as the maximum modulus of $\boldsymbol{a}$ at a Sun-spacecraft reference distance $r_\oplus \triangleq 1\,\mathrm{au}$, τ is a dimensionless (voltage) parameter that models the thrust modulation by suitably adjusting the tether voltage, and $\gamma = \gamma(\alpha_n)$ is the dimensionless propulsive acceleration defined as the ratio of the local value of $\|\boldsymbol{a}\|$ at a certain pitch angle α_n to the local maximum propulsive acceleration. In Eq. (1), the thrust direction is given by the propulsive acceleration unit vector $\hat{\boldsymbol{a}}$ that, according to Ref. [14], forms an angle $\alpha = \alpha(\alpha_n) \in [0,\, 90]\,\mathrm{deg}$ (the so called cone angle) with the Sun-spacecraft direction $\hat{\boldsymbol{r}}$.

The variation [14] of both the dimensionless propulsive acceleration γ and the cone angle α with the sail pitch angle α_n is shown in Fig. 2. In particular, the cone angle has a nearly linear variation with the pitch angle (in the form $\alpha \simeq \alpha_n/2$) if $\alpha_n \leq 20\,\mathrm{deg}$, whereas the function $\alpha = \alpha(\alpha_n)$ is nonlinear if $\alpha_n > 20\,\mathrm{deg}$ and reaches a maximum value of about $20\,\mathrm{deg}$ when $\alpha_n \simeq 55\,\mathrm{deg}$. On the other hand, the dimensionless propulsive acceleration is maximum ($\gamma = 1$) at $\alpha_n = 0$, i.e. when $\hat{\boldsymbol{r}} = \hat{\boldsymbol{n}}$, and then decreases monotonically with the pitch angle. For an in depth analysis of the thrust mathematical model for mission analysis purposes, the interested reader is referred to Refs. [15, 18].

2.1. Equations of motion

The dynamics of the spacecraft, which covers a DNKO of given characteristics, can be conveniently described in the cylindrical reference frame $\mathcal{T}_c\,(O; \rho,\, \theta,\, z)$ through the following equations of motion

$$\ddot{\rho} = \rho\,\dot{\theta}^2 - \frac{\mu_\odot}{r^3}\,\rho + a_\rho \tag{2}$$

$$\ddot{\theta} = -\frac{2\,\dot{\rho}\,\dot{\theta}}{\rho} \tag{3}$$

$$\ddot{z} = -\frac{\mu_\odot}{r^3}\,z + a_z \tag{4}$$

where $\mu_\odot$ is the Sun's gravitational parameter, a_ρ and a_z are the radial (along the O'-S direction) and vertical (along the z-axis) components of the spacecraft propulsive acceleration $\boldsymbol{a}$. Taking into account Eq. (1) and Fig. 3, the expressions of a_ρ and a_z are

$$a_\rho = \tau\, a_c \left(\frac{r_\oplus}{r}\right) \gamma\, \cos\left(\alpha + \psi\right) \tag{5}$$

$$a_z = \tau\, a_c \left(\frac{r_\oplus}{r}\right) \gamma\, \sin\left(\alpha + \psi\right) \tag{6}$$

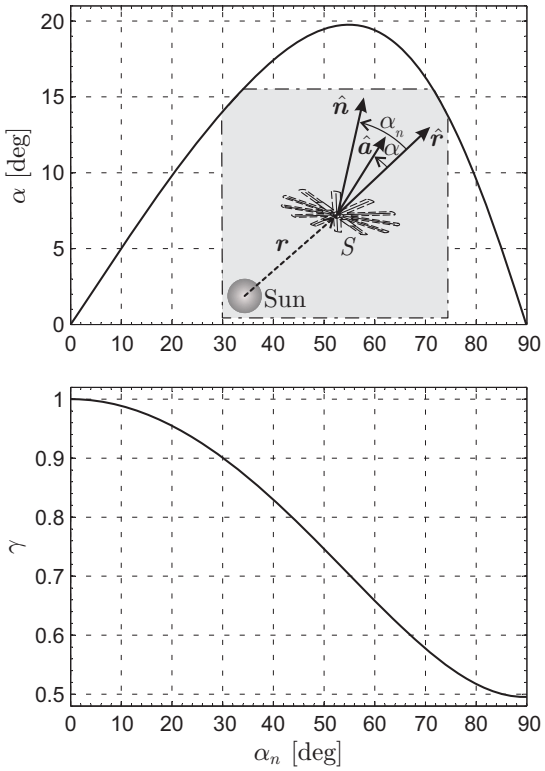

Figure 2: E-sail cone angle α and dimensionless propulsive acceleration γ as a function of the sail pitch angle α_n.

where $\psi \in [0,\, 90]\,\mathrm{deg}$ is the spacecraft elevation angle, see also Fig. 1, defined as the angle between the direction of $\hat{\boldsymbol{r}}$ and the planet's orbital plane (x, y), viz.

$$\psi = \arcsin\left(\frac{H}{r}\right) \equiv \arccos\left(\frac{\rho}{r}\right) \tag{7}$$

Note that ψ is a function of both the characteristics of the DNKO, and the spacecraft position around the orbit through the distance r from the Sun's center-of-mass. In particular, the limit case of $\psi = 0$ (or $H = 0$) refers to a situation in which the spacecraft and the celestial body cover two coplanar orbits. Moreover, it is interesting to observe that the E-sail does not require any circumferential acceleration component for the DNKO maintenance. In fact, the E-sail thrust generates a net force acting on the spacecraft which is identical to the one of a attractor body, whose center-of-mass is placed just in O', so that the DNKO has an identical shape with respect to the corresponding Keplerian orbit. This can be obtained only if there is not a circumferential component of the resultant force.

Equation (3) can be easily integrated to yield

$$h_z \triangleq \dot{\theta}\,\rho^2 = \text{constant} \tag{8}$$

where h_z is the component along the z-axis of the classical spacecraft specific angular momentum $\boldsymbol{h} = \boldsymbol{r} \times \boldsymbol{v}$, and $\boldsymbol{v}$ is the spacecraft inertial velocity vector. Note that h_z coincides with the modulus of the spacecraft specific angular momentum calculated with respect to the DNKO focus O'. Bearing in mind Eqs. (5)-(6) and (8), the two equations of motion (2) and (4) can be rewritten as

$$\ddot{\rho} = \frac{h_z^2}{\rho^3} - \frac{\mu_\odot}{r^3}\rho + \tau\, a_c \left(\frac{r_\oplus}{r}\right) \gamma\, \cos\left(\alpha + \psi\right) \tag{9}$$

$$\ddot{z} = -\frac{\mu_\odot}{r^3}\, z + \tau\, a_c \left(\frac{r_\oplus}{r}\right) \gamma\, \sin\left(\alpha + \psi\right) \tag{10}$$

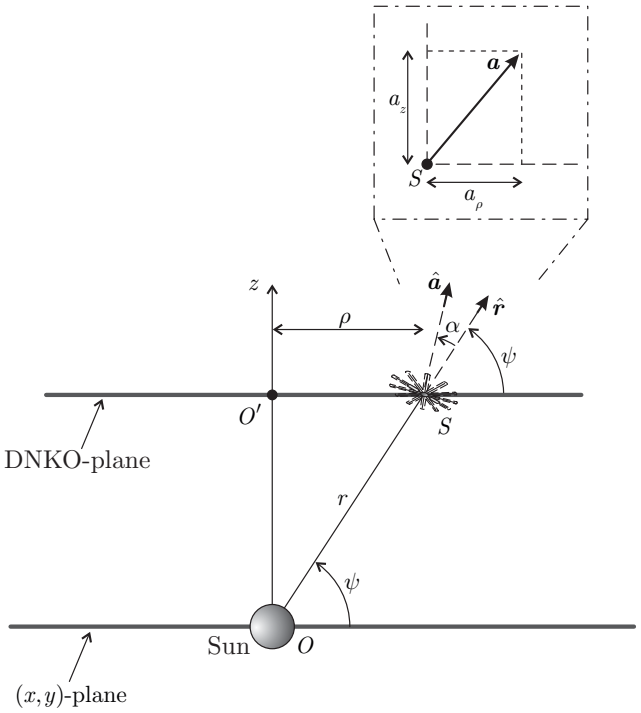

Figure 3: Components of the spacecraft propulsive acceleration.

where ψ is given by Eq. (7). The Eqs. (9)-(10) are now used to analyze special families of DNKOs of practical interest.

3. Planet following displaced orbits

An interesting mission scenario consists in generating a displaced orbit in which the spacecraft belongs, at any time, to the plane $\mathcal{P}$ defined by the Sun's position, the planet's position, and the point O', see Fig. 4. Such a DNKO is particularly useful from a scientific point of view, because this orbit allows the spacecraft to "overfly" the polar zones of the planet at all times, assuming that the inclination of the planetary axis with respect to the heliocentric orbital plane is neglected.

A straightforward strategy to meet such a condition is to enforce that both the spacecraft and the planet transit simultaneously at their perihelion (P' and P, respectively) and generate a DNKO having: i) a displacement H from the celestial body's orbital plane; ii) the same eccentricity e of the (Keplerian) planet's orbit; iii) the perihelion P' such that the segment O'-P' is parallel to x-axis (i.e. $\omega = 0$, see Fig. 1). This particular DNKO will now be referred to as Planet Following Displaced Orbit (PFDO), see Fig. 4.

Note that in a PFDO the planet's true anomaly ν matches θ at any time, and the ratio q between the O'-spacecraft distance ρ and the O-planet distance r_p

$$q \triangleq \frac{\rho}{r_p} \tag{11}$$

is a constant of motion. In particular, in this scenario the dimensionless parameter q can be viewed as the ratio between the semimajor axis of the spacecraft orbit and that of the planet's heliocentric orbit. Therefore, to maintain the PFDO, the two constraints to be met are

$$\frac{\mathrm{d}^2 q}{\mathrm{d}\nu^2} = 0 \tag{12}$$

$$\ddot{z} = 0 \tag{13}$$

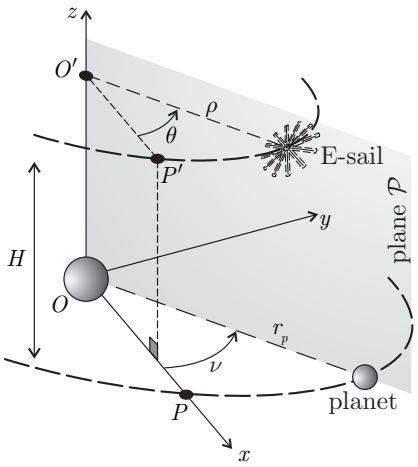

Figure 4: Schematic view of a planet following displaced orbit (PFDO).

where Eq. (13) guarantees that the PFDO orbital plane is parallel to the (x, y) plane at any time. Paralleling the discussion of Gong and Li [19], it can be verified that the second derivative of q with respect to the true anomaly $\nu \equiv \theta$ can be written as

$$\frac{\mathrm{d}^2 q}{\mathrm{d}\nu^2} = \frac{1}{1 + e\cos\nu}\left[q\left(1 - \frac{r_p^3}{r^3}\right) + \frac{a_\rho}{\mu_\odot / r_p^2}\right] \tag{14}$$

Taking into account Eq. (7), Eqs. (12) and (14) provide the expression of the component a_ρ of the propulsive acceleration required to maintain the PFDO of given values of H and q

$$a_\rho = \frac{\mu_\odot}{r_p^2}\, q\left(\frac{\cos^3\psi}{q^3} - 1\right) \tag{15}$$

whereas, from Eqs. (10) and (13), the vertical component a_z of the required propulsive acceleration is obtained as

$$a_z = \frac{\mu_\odot}{r_p^2}\,\frac{\cos^2\psi\,\sin\psi}{q^2} \tag{16}$$

Note that the values of both a_ρ and a_z depend on the spacecraft position on the PFDO through the distance r in the expression of the elevation angle ψ, see Eq. (7). A special case is when both the PFDO and the planet's orbits are circular ($e = 0$) and r is a constant of motion. In that case, a thoroughly analysis of this scenario is discussed in Ref. [16].

As is implied by Eqs. (15)-(16), for a given planet's (reference) orbit, the propulsive requirements necessary to maintain a PFDO depend on the constant parameter q and, therefore, on the semimajor axis of the spacecraft orbit. These propulsive requirements must be compared against the limits related to the E-sail behavior, in particular, its maximum cone angle $\alpha_{\max} \simeq 19.75\,\mathrm{deg}$, see Fig. 2. In what follows, two different mission cases will be discussed, depending on the chosen value of the ratio q.

3.1. Case of $q = 1$: the "levitating" spacecraft.

Assume the PFDO semimajor axis be equal to that of the reference planet's orbit or, equivalently, assume that $q = 1$. This implies that the PFDO is obtained by a rigid displacement (equal to H) of the planet's orbit along the z-axis. This particular condition allows the spacecraft to be always along the celestial body's vertical, at a distance H from its center of mass. This means that the spacecraft "levitates" above (or below, depending on the direction of the rigid displacement) the celestial body, see Fig. 5.

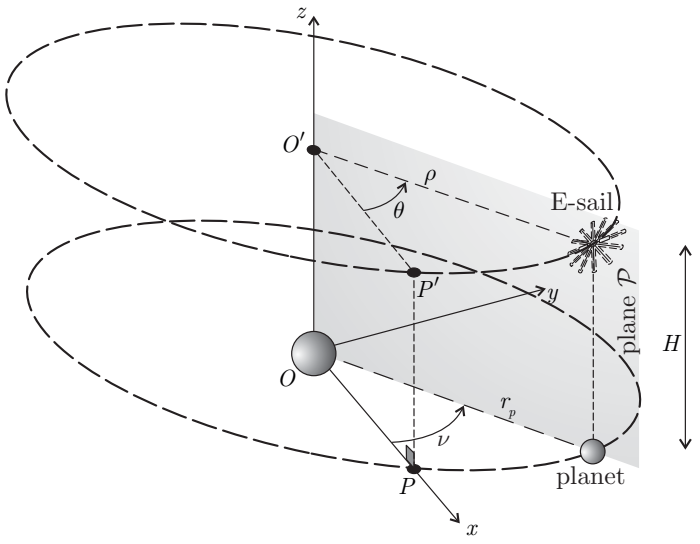

Figure 5: Scheme of a PFDO with $q = 1$: the "levitating" spacecraft.

From a mathematical viewpoint, the levitating condition is obtained when $q = 1$ in the previous dynamical model. Therefore, recalling Eqs. (5)-(6), the conditions for orbital maintenance Eqs. (15)-(16) become

$$a_\rho = \tau\, a_c \left(\frac{r_\oplus}{r}\right) \gamma\, \cos\left(\alpha + \psi\right) = \frac{\mu_\odot}{r_p^2}\, \left(\cos^3\psi - 1\right) \tag{17}$$

$$a_z = \tau\, a_c \left(\frac{r_\oplus}{r}\right) \gamma\, \sin\left(\alpha + \psi\right) = \frac{\mu_\odot}{r_p^2}\, \cos^2\psi\, \sin\psi \tag{18}$$

Note that the radial component of the propulsive acceleration a_ρ for $\psi \neq 0$ is always negative, that is, the propulsive acceleration vector $\boldsymbol{a}$ points towards the inner part of the spacecraft orbit.

In this case, the cone angle α required for orbital maintenance at a generic spacecraft angular position $\theta \equiv \nu$ can be calculated by taking the ratio of Eqs. (17) to (18). Accordingly, for a given value of H, the cone angle can be written as a function of ν (or θ) as

$$\alpha = \arctan\left(\frac{\cos^2\psi\, \sin\psi}{\cos^3\psi - 1}\right) - \psi \tag{19}$$

where, in this scenario, ψ can be conveniently expressed as a function of the characteristics $\{a,\, e\}$ of the planet's orbit as

$$\psi = \arctan\left(\frac{H}{r_p}\right) \tag{20}$$

where r_p is given, as a function of the true anomaly ν, by the planet's orbit polar equation

$$r_p = \frac{a\, \left(1 - e^2\right)}{1 + e\cos\nu} \tag{21}$$

The variation of the cone angle α with the elevation angle ψ, as described by Eq. (19), is shown in Fig. 6. This figure demonstrates that, unfortunately, the values of α, when $q = 1$ and the spacecraft levitates over the planet, are well beyond the E-sail intrinsic limit of about 20 deg, see Fig. 2.

In fact, taking into account for example two practical mission scenario, Figs. 7(a) and 7(b) show the required values of α as a function of the PFDO true anomaly $\theta \equiv \nu \in [0,\, 360]$ deg for different altitudes $H \in [0.01,\, 1]$ au above Earth ($a = 1.000$ au, and $e = 0.167$) and Mercury ($a = 0.387$ au, and $e = 0.206$), respectively.

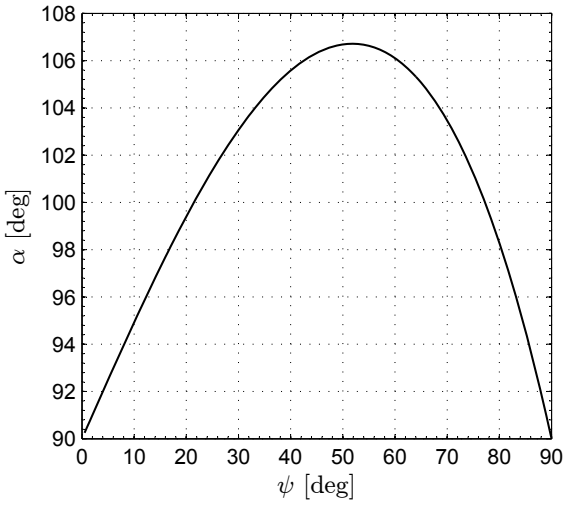

Figure 6: Required cone angle, as a function of the elevation angle, for a PFDO with $q = 1$.

The simplification that could be obtained using a circular PFDO, with a constant elevation angle and therefore a constant cone angle, does not change substantially the situation [16]. Therefore, this particular kind of elliptic DNKO cannot be maintained by an E-sail according to the advanced thrust model of Ref. [14]. However, the propulsive requirements for a PFDO can be reduced to feasible values for an E-sail by adopting a displaced orbit with a semimajor axis smaller than the one of the reference planetary orbit, as is now discussed.

3.2. Case of $q < 1$: the shrunk PFDO.

A possibility for avoiding the problems highlighted in the previous section consists in the generation of a sort of "shrunk" PFDO, that is, a displaced orbit with the same eccentricity e of the planetary orbit, but with a smaller semimajor axis, see Fig. 8.

With such a choice the equilibrium condition given by Eq. (12) still holds, and Eq. (15) still provides the radial component a_ρ of the propulsive acceleration. However, in this case $q < 1$ and, therefore, a_ρ can take a positive value because $\cos\psi \geq q$, or $r \leq r_p$, see the sketch in Fig. 8. The equilibrium equations are therefore

$$a_\rho = \tau\, a_c \left(\frac{r_\oplus}{r}\right) \gamma\, \cos\left(\alpha + \psi\right) = \frac{\mu_\odot}{r_p^2}\, q \left(\frac{\cos^3\psi}{q^3} - 1\right) \tag{22}$$

$$a_z = \tau\, a_c \left(\frac{r_\oplus}{r}\right) \gamma\, \sin\left(\alpha + \psi\right) = \frac{\mu_\odot}{r_p^2}\, \frac{\cos^2\psi\, \sin\psi}{q^2} \tag{23}$$

which generalize Eqs. (17)-(18) when $q \neq 1$.

Combining Eqs. (22) and (23), the cone angle required for PFDO maintenance is

$$\alpha = \arctan\left(\frac{\cos^2\psi\, \sin\psi}{\cos^3\psi - q^3}\right) - \psi \tag{24}$$

and the voltage parameter is

$$\tau = \frac{\mu_\odot\, q}{a_c\, \gamma\, r_\oplus\, r_p\, \cos\psi} \sqrt{q^2 + \frac{\cos^4\psi}{q^4} - 2\,\frac{\cos^3\psi}{q}} \tag{25}$$

Note that both α and τ (that accounts for the possibility of varying the grid voltage to modulate the E-sail thrust modulus) are functions of the ratio q.

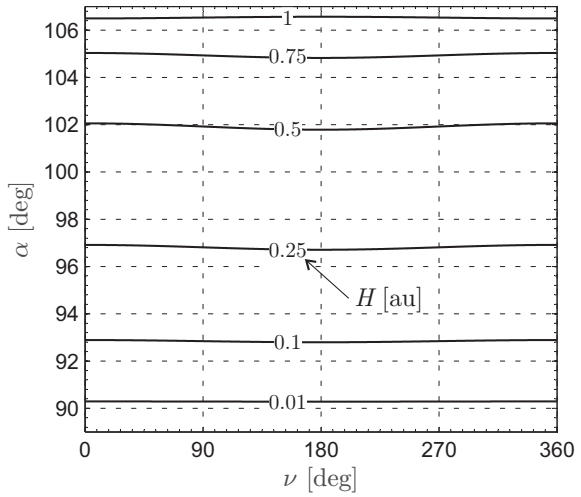

(a) Earth scenario.

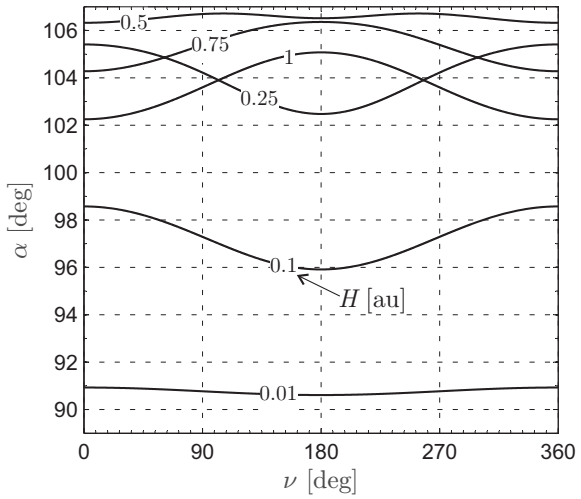

(b) Mercury scenario.

Figure 7: Required cone angle α as a function of the true anomaly ν and orbit displacement H for a PFDO with $q = 1$ (the case of a the "levitating" spacecraft).

According to Eq. (24), the variation of the required cone angle α with the elevation angle ψ and the ratio q is shown in Fig. 9. In this case, reducing the values of the dimensionless quantity q allows orbital maintenance of displaced orbits whose characteristics are compatible with the E-sail propulsive constraints in terms of $\alpha \leq \alpha_{\max}$, see also Fig. 2.

In particular, enforcing in Eq. (24) the propulsive constraint $\alpha \leq \alpha_{\max}$, it is possible to obtain the admissible range of the elevation angle as a function of the value of q. The result, in terms of an allowable region in the (q, ψ) plane, is shown in Fig. 10. Note that in the limit case of $q = 1$, the allowable interval of elevation angle collapse in a point, i.e. $\psi = 0$. This condition refers to a DNKO with $H = 0$, that is, an orbit coplanar to the planet's orbital plane. Indeed, as discussed before, the scenario of a PFDO in which $q = 1$ is unfeasible from the point of view of the sail cone angle constraint $\alpha \leq \alpha_{\max}$.

To summarize, for a given planet's orbital characteristics $\{a, e\}$ and a given value of the triplet $\{H,\, q,\, \nu\}$, the elevation angle is given by

$$\psi = \arctan\left(\frac{H}{q\, r_p}\right) \equiv \arctan\left[\frac{H\ (1 + e\, \cos\nu)}{q\, a\ (1 - e^2)}\right] \tag{26}$$

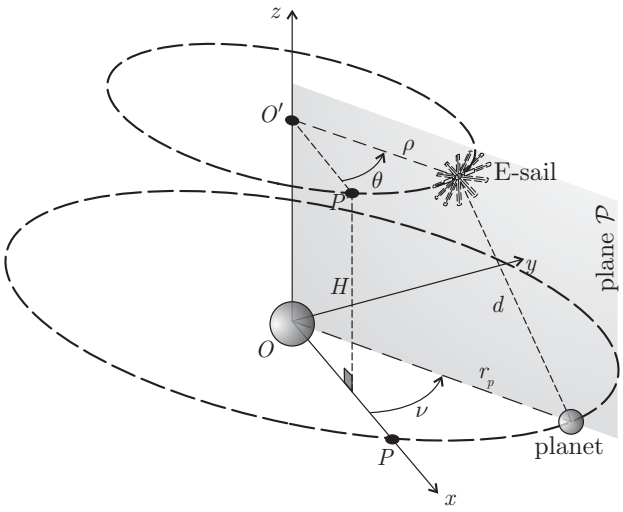

Figure 8: Scheme of a PFDO with $q < 1$: the "shrunk" displaced orbit.

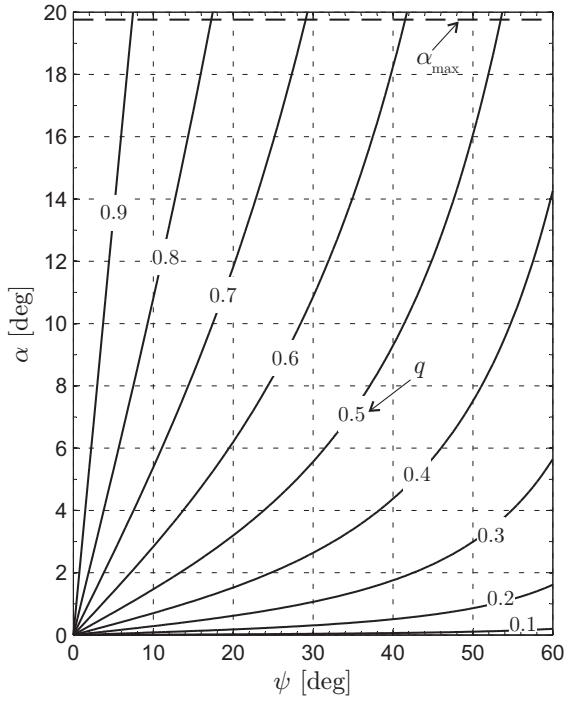

Figure 9: Required cone angle, as a function of the elevation angle and the ratio q, for a shrunk PFDO.

and the required cone angle α is given by Eq. (24). The sail pitch angle α_n and the dimensionless propulsive acceleration γ are obtained, as a function of α, from Fig. 2 and, finally, the propulsive requirements $\tau\, a_c$ are calculated from Eq. (25), where the value of r_p is obtained from Eq. (21). Note that $\tau\, a_c$ is actually the product of a fixed value (a_c), which characterizes the E-sail performance, and a varying parameter (τ), which accounts for the thrusting variation throughout the orbit. Typically, in a preliminary phase of mission design, the mean value of $\tau\, a_c$ is chosen equal to the characteristic acceleration requirement for orbital maintenance, while the tether voltage is varied along the orbit according to the control law given by Eq. (25).

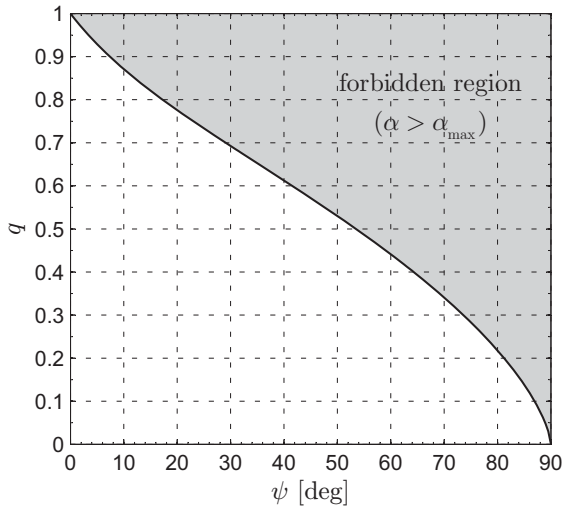

Figure 10: Allowable region in the (q, ψ) plane for a shrunk PFDO.

From the point of view of the value of the characteristic acceleration, preliminary studies suggest that a shrunk PFDO could be easily generated and maintained, using an E-sail with medium-low performances (i.e. $a_c < 1\,\mathrm{mm/s^2}$), in mission scenarios involving Earth, Venus, or Mars. For example, Tab. 1 summarizes the orbital characteristics of three potential shrunk PFDOs, with the same value of ratio $q = 0.99$, for a medium-low performance E-sail. The distance between the spacecraft and the planet's center of mass is indicated with d (see Fig. 8). Its maximum ($d_{\max}$) and minimum ($d_{\min}$) values are shown in the last two columns for the potential shrunk PFDO mission scenarios. Note that the difference between the two values is larger, as expected, if the planet has a not-negligible (heliocentric) orbital eccentricity.

Planet	$a_c\,[\mathrm{mm/s^2}]$	q	$H\,[\mathrm{au}]$	$d_{\min}\,[\mathrm{au}]$	$d_{\max}\,[\mathrm{au}]$
Venus	0.370	0.99	0.0075	0.0104	0.0105
Earth	0.260	0.99	0.0100	0.0140	0.0143
Mars	0.167	0.99	0.0130	0.0190	0.0211

Table 1: Characteristics of potential shrunk PFDOs for a medium-low performance E-sail.

The variation of both the sail pitch angle α_n and the voltage parameter τ with the planet's true anomaly ν (recall that, in a shrunk PFDO the condition $\theta \equiv \nu$ holds) is shown in Figs. 11-13. In particular, the voltage parameter is shown as a ratio to the mean value $\overline{\tau}$ over the true anomaly range. Note that the voltage parameter τ shows a variation around the mean value $\overline{\tau}$ along the orbit which is quite small for the analyzed mission scenario. This variation is of the order of $1\% - 2\%$ for Earth and Venus cases, and of 10% for Mars case. A similar consideration can be made for α_n, which shows an oscillation of few degrees around the mean value throughout the whole orbit.

The variation of both α_n and τ with ν is (qualitatively) invariant with respect to a change in the value of q. For example, Fig. 14 shows the required pitch angle and voltage parameter, in a Mercury scenario, with an high performance E-sail ($a_c = 2.37\,\mathrm{mm/s^2}$) and a ratio $q = 0.97$. In this case, however, a considerable variation over the orbit of both the sail pitch angle (about 20 deg), and the voltage parameter (about 30% of the mean value $\overline{\tau}$) are required to maintain the displaced heliocentric trajectory.

4. Conclusions

The analysis presented in this work shows that the Electric Solar Wind Sail, an innovative and exotic propulsion concept, largely different from the classic photonic solar sail, is capable of generating elliptic,

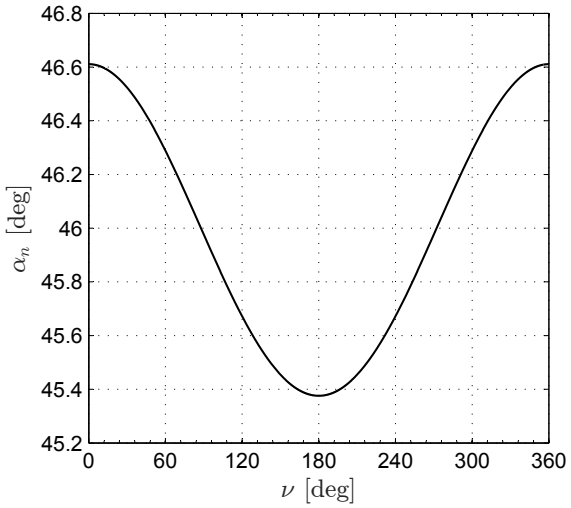

(a) Pitch angle α_n.

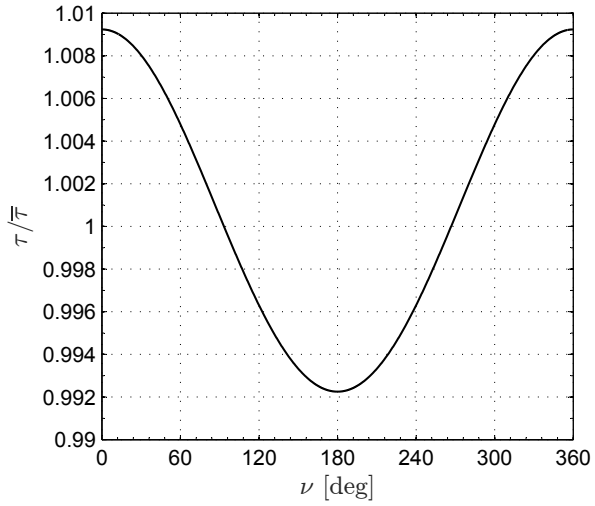

(b) Voltage parameter τ

Figure 11: Angular variation of the pitch angle and voltage parameter for a shrunk PFDO above Venus, with $H = 0.0075\,\text{au}$, $q = 0.99$, and $a_c = 0.320\ \text{mm/s}^2$.

heliocentric, displaced orbits. In particular, the intrinsic capability of such a propulsion system of varying the magnitude of the thrust by adjusting the tethers voltage (within certain limits) makes the Electric Solar Wind Sail particulary suitable to maintain a displaced non-Keplerian orbit.

However, the physical constraint related to the maximum cone angle, which cannot exceed few tens of degrees, is an important limitation for the characteristics (semimajor axis, eccentricity, and displacement) of the displaced trajectories that can be generated and maintained. In this context, this study provides specific mathematical tools, in terms of analytical expressions and calculation algorithms, useful to quickly identify the elliptic displaced orbits that can be effectively maintained by a spacecraft equipped with an Electric Solar Wind Sail of given characteristics.

Using the mathematical model discussed in this work, it has been observed that some special elliptic displaced orbits, in particular the ones that allow the levitation of the spacecraft above the planet's zenith (or nadir), are physically impossible to maintain using an Electric Solar Wind Sail apart from the value of the characteristic acceleration, because of the cone angle constraint. However, the model has shown that it is

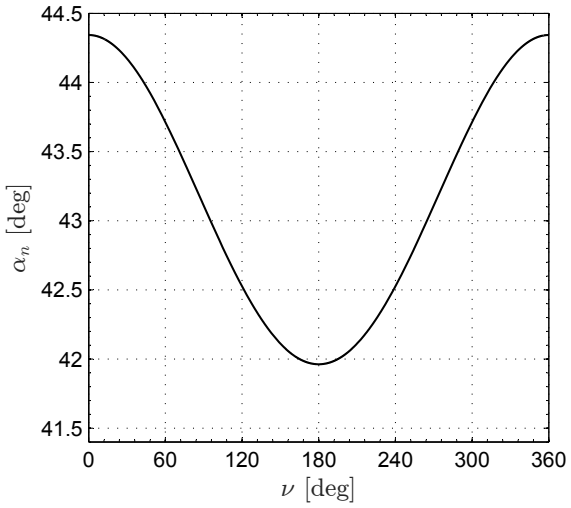

(a) Pitch angle α_n.

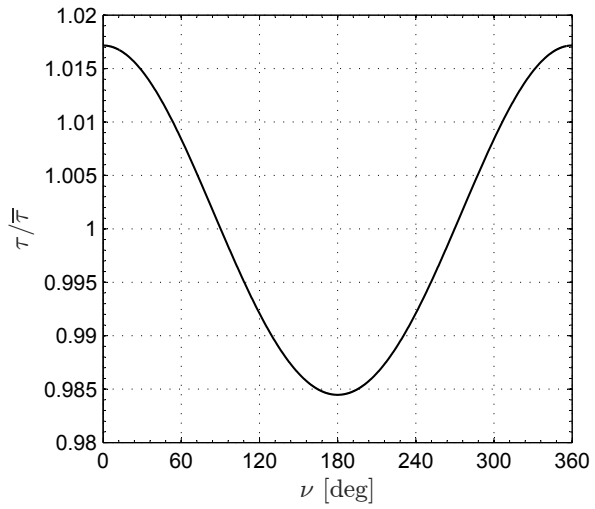

(b) Voltage parameter τ

Figure 12: Angular variation of the pitch angle and voltage parameter for a shrunk PFDO above Earth, with $H = 0.01$ au, $q = 0.99$, and $a_c = 0.260$ mm/s^2.

possible to generate interesting trajectories with a low-medium performance propulsive system, by relaxing the condition on the relative vertical position of spacecraft with respect to the planet (the so called shrunk orbits).

A natural extension of this work could be a study that accounts for the axial inclination of the planets with respect to their orbital planes. A not negligible inclination could allow an observation of the planet's North (South) Pole with an optimal view angle at summer (winter) solstice, if the spacecraft is placed above (below) the planet's orbital plane, on a shrunk PFDO having a specific value of the ratio q. On the other hand, at winter (summer) solstice the view angle would be the largest throughout the whole orbit. However, the opportunity of having a line of sight from the spacecraft to a planet's pole with a small view angle during a whole season could deserve further investigations. Another possible improvement to this analysis consists in the inclusion of the planetary gravity in the model. This effect would not be significant for the orbits studied in this paper, which are outside the planetary spheres of influence, but could be important for the study of DNKOs sufficiently close to the planet's poles.

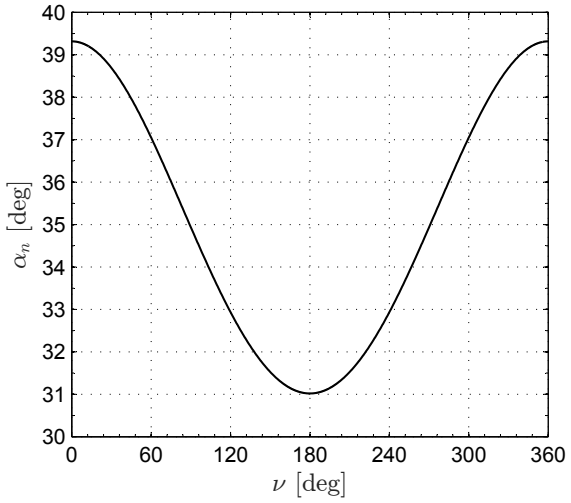

(a) Pitch angle α_n.

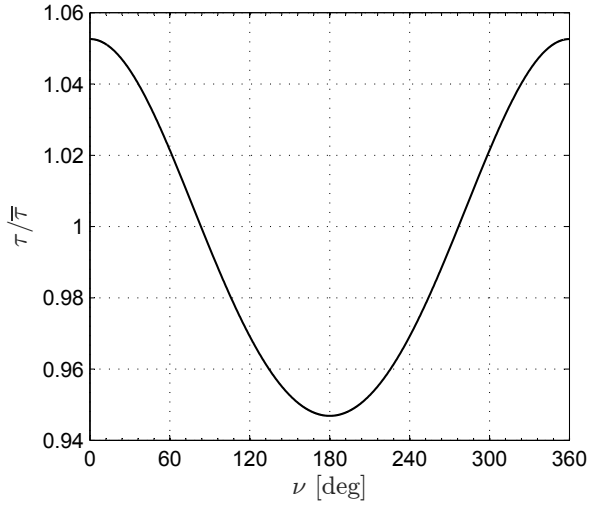

(b) Voltage parameter τ

Figure 13: Angular variation of the pitch angle and voltage parameter for a shrunk PFDO above Mars, with $H = 0.013\,\text{au}$, $q = 0.99$, and $a_c = 0.167\ \text{mm/s}^2$.

References

[1] P. Janhunen, Electric sail for spacecraft propulsion, Journal of Propulsion and Power 20 (4) (2004) 763–764, doi: 10.2514/1.8580.

[2] P. Janhunen, A. Sandroos, Simulation study of solar wind push on a charged wire: basis of solar wind electric sail propulsion, Annales Geophysicae 25 (3) (2007) 755–767, doi: 10.5194/angeo-25-755-2007.

[3] P. Janhunen, P. K. Toivanen, J. Polkko, S. Merikallio, P. Salminen, E. Haeggström, H. Seppänen, R. Kurppa, J. Ukkonen, S. Kiprich, G. Thornell, H. Kratz, L. Richter, O. Krömer, R. Rosta, M. Noorma, J. Envall, S. Lätt, G. Mengali, A. A. Quarta, H. Koivisto, O. Tarvainen, T. Kalvas, J. Kauppinen, A. Nuottajärvi, A. Obraztsov, Electric solar wind sail: Toward test missions, Review of Scientific Instruments 81 (11) (2010) 111301–1–11301–11, doi: 10.1063/1.3514548.

[4] P. Toivanen, P. Janhunen, Spin plane control and thrust vectoring of electric solar wind sail, Journal of Propulsion and Power 29 (1) (2013) 178–185, doi: 10.2514/1.B34330.

[5] P. Janhunen, Coulomb drag devices: electric solar wind sail propulsion and ionospheric deorbiting, Space Propulsion 2014, Köln, Germany, 2014, paper SP2014_2969331, Session 80.

[6] G. Mengali, A. A. Quarta, P. Janhunen, Electric sail performance analysis, Journal of Spacecraft and Rockets 45 (1) (2008) 122–129, doi: 10.2514/1.31769.

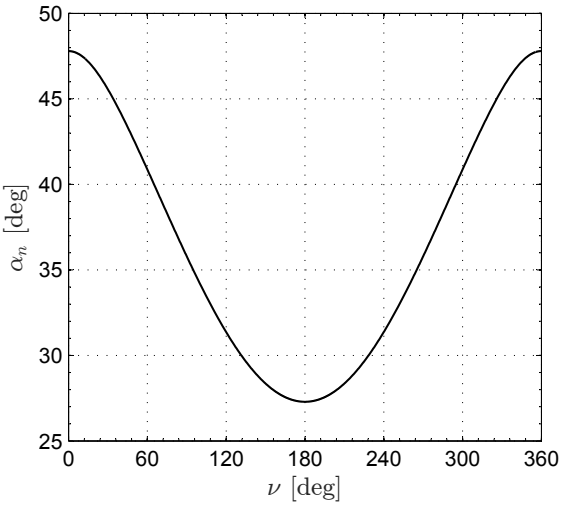

(a) Pitch angle α_n.

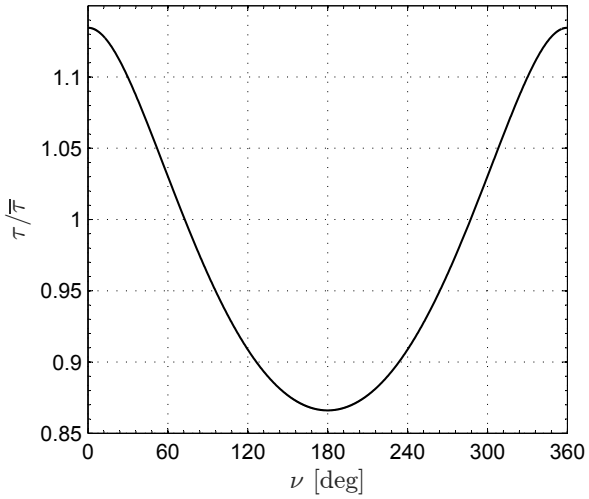

(b) Voltage parameter τ

Figure 14: Angular variation of the pitch angle and voltage parameter for a shrunk PFDO above Mercury, with $H = 0.01$ au, $q = 0.97$, and $a_c = 2.370$ mm/s^2.

[7] P. Janhunen, A. A. Quarta, G. Mengali, Electric solar wind sail mass budget model, Geoscientific Instrumentation, Methods and Data Systems 2 (1) (2013) 85–95, doi: 10.5194/gi-2-85-2013.

[8] C. R. McInnes, Dynamics, stability, and control of displaced non-keplerian orbits, Journal of Guidance, Control, and Dynamics 21 (5) (1998) 799–805, doi: 10.2514/2.4309.

[9] M. MacDonald, R. J. McKay, M. Vasile, F. De Frescheville, J. D. Biggs, C. R. McInnes, Low-thrust-enabled highly-non-keplerian orbits in support of future mars exploration, Journal of Guidance, Control, and Dynamics 34 (5) (2011) 1396–1411, doi: 10.2514/1.52602.

[10] J. Heiligers, C. R. McInnes, New families of sun-centred non-keplerian orbits over cylinders and spheres, Celestial Mechanics and Dynamical Astronomy 120 (2) (2014) 163–194, doi: 10.1007/s10569-014-9570-7.

[11] R. J. McKay, M. Macdonald, J. D. Biggs, C. R. McInnes, Survey of highly-non-keplerian orbits with low-thrust propulsion, Journal of Guidance, Control, and Dynamics 34 (3) (2011) 645–666, doi: 10.2514/1.52133.

[12] G. Mengali, A. A. Quarta, Non-Keplerian orbits for electric sails, Celestial Mechanics and Dynamical Astronomy 105 (1–3) (2009) 179–195, doi: 10.1007/s10569-009-9200-y.

[13] P. Janhunen, The electric solar wind sail status report, in: European Planetary Science Congress 2010, Vol. 5, European Planetology Network and the European Geosciences Union, 2010, paper EPSC 2010-297.

[14] K. Yamaguchi, H. Yamakawa, Study on orbital maneuvers for electric sail with on-off thrust control, Aerospace Technology Japan 12 (2013) 79–88, doi: 10.2322/astj.12.79.

[15] K. Yamaguchi, H. Yamakawa, Electric solar wind sail kinetic energy impactor for near earth asteroid deflection mission, The Journal of the Astronautical Sciences 63 (1) (2016) 1–22, doi: 10.1007/s40295-015-0081-x.
[16] L. Niccolai, A. A. Quarta, G. Mengali, Electric sail-based displaced orbits with a refined thrust model, (submitted). Proceedings of the Institution of Mechanical Engineers, Part G: Journal of Aerospace Engineering .
[17] P. Toivanen, P. Janhunen, J. Envall, Electric sail control mode for amplified transverse thrust, Acta Astronautica 106 (2015) 111–119, doi: 10.1016/j.actaastro.2014.10.031.
[18] A. A. Quarta, G. Mengali, Minimum-time trajectories of electric sail with advanced thrust model, Aerospace Science and Technology, 55 (2016) 419–430, doi: 10.1016/j.ast.2016.06.020.
[19] S. Gong, J. Li, Solar sail heliocentric elliptic displaced orbits, Journal of Guidance, Control, and Dynamics 37 (6) (2014) 2021–2025, doi: 10.2514/1.G000660.